Lipids in Health and Disease

RESEARCH

Open Access

Fucoidan ameliorates lipid accumulation, oxidative stress, and NF-κB-mediated inflammation by regulating the PI3K/AKT/Nrf2 signaling pathway in a free fatty acid-induced NAFLD spheroid model

Xueru Chu[1], Xuan Wang[1], Keqing Feng[1], Yanzhen Bi[2], Yongning Xin[1,2*] and Shousheng Liu[3*]

Abstract

Background Non-alcoholic fatty liver disease (NAFLD) is the most prevalent chronic liver disease worldwide. Previous studies have reported that fucoidan can relieve obesity and hepatic steatosis in vivo, although the molecular mechanism remains unclear. This study aimed to explore the effect and potential molecular mechanism of fucoidan in NAFLD using the free fatty acid (FFA)-induced NAFLD spheroid model.

Materials and methods The spheroids were constructed by fusing the HepG2 and LX-2 cells. Spheroids and HepG2 cells were stimulated with FFAs and fucoidan, then the intracellular lipid contents and the oxidative stress levels (ROS/MDA/GSH/GR/GPx/NQO1/GCLC/HO-1) were detected. Furthermore, the regulation of PI3K/AKT/Nrf2 pathway and the expression of inflammatory factors (TNF-α and IL-6) were measured.

Results Fucoidan markedly reduced FFA-induced intracellular lipid accumulation in spheroids and HepG2 cells. Notably, fucoidan relieved FFA-induced oxidative stress by reducing the levels of ROS and MDA, and elevating the levels of GSH, GR, and GPx. Furthermore, fucoidan reduced FFA-induced oxidative stress by activating the PI3K/AKT/Nrf2 signaling pathway and by inhibiting ROS-induced P65 NF-κB activation and inflammatory responses via Nrf2 pathway activation.

Conclusions Our results demonstrated that fucoidan ameliorated FFA-induced lipid accumulation, oxidative stress, and NF-κB-mediated inflammation through the PI3K/AKT/Nrf2 signaling pathway in the spheroid and HepG2 cells model of NAFLD. These results provided new evidence for the clinical use of fucoidan in the treatment of NAFLD and its potential molecular mechanism of action.

Keywords Non-alcoholic fatty liver disease, Fucoidan, Spheroid, Lipid accumulation, Oxidative stress

*Correspondence:
Yongning Xin
xinyongning@163.com
Shousheng Liu
shoushengliuouc@163.com

[1]School of Medicine and Pharmacy, Ocean University of China, Department of Infectious Disease, Qingdao Municipal Hospital, Qingdao 266011, China
[2]Department of Infectious Disease, Qingdao Municipal Hospital, 1 Jiaozhou Road, Qingdao, Shandong Province 266011, China
[3]Clinical Research Center, Qingdao Municipal Hospital, 5 Donghaizhong Road, Qingdao, Shandong Province 266011, China

Introduction

The prevalence of non-alcoholic fatty liver disease (NAFLD) has increased from 25 to 38% over the past 30 years [1–3]. As a multisystem metabolic disease, NAFLD is closely associated with obesity, type 2 diabetes mellitus, insulin resistance and so on [4–6]. Non-alcoholic steatohepatitis (NASH) is a progressive stage defined as hepatic steatosis and chronic inflammation with or without fibrosis [7]. On March 14, 2024, Rezdiffra™ (resmetirom) became the first drug approved to treat NASH by the U.S. Food and Drug Administration (https://www.madrigalpharma.com/). Aside from this, no other targeted drugs are available for the treatment of NAFLD, likely because the pathogenesis of NAFLD is complex and is not fully elucidated. Therefore, it is particularly urgent to elucidate the pathogenesis of NAFLD in order to develop targeted therapeutic drugs.

Recently, a new theory called the "multiple hits" hypothesis has provided a more appropriate description of the pathogenesis of NAFLD, pointing to insulin resistance, mitochondrial dysfunction, endoplasmic reticulum stress, and alterations in gut microbial functions as major contributors to the pathogenesis of NAFLD [8]. Oxidative stress is one of the factors leading to these "multiple hits", thus it is regarded as the main cause of NAFLD-related liver injury and disease progression [9, 10]. In the pathological condition of NAFLD, excess mitochondrial reactive oxide species (ROS) can lead to oxidative stress and the formation of lipid peroxides, such as malondialdehyde (MDA) and 4-hydroxynonenal [11]. Excessive accumulation of ROS can activate hepatic nuclear factor kappa-B (NF-κB)-mediated inflammatory pathways and promote the expression of inflammatory cytokines, such as tumor necrosis factor-α (TNF-α) and interleukin-6 (IL-6) [12–14]. The secretion of inflammatory cytokines can further activate intrahepatic macrophages and hepatic stellate cells, leading to inflammatory cell recruitment and liver fibrosis [15]. Therefore, screening of drugs and food additives focus on inhibiting oxidative stress and ROS overproduction can provide critical insight in the treatment of NAFLD.

Fucoidan is often used as a food supplement due to its reported beneficial nutritional and health properties [16]. Accumulated studies have reported the many health benefits of fucoidan, as an anti-oxidant and as an anti-inflammatory, lipid-lowering, and liver protective mediator [17–19]. The in vivo protective effects of fucoidan on high-fat diet (HFD)-induced hepatic steatosis and obesity have been reported, however the exact mechanism of action of fucoidan in HFD-induced steatosis and NAFLD remains unclear [20, 21]. In recent years, three-dimensional (3D) cell models have aroused great interests for their research superiority compared to the traditional two-dimensional cell models. The spheroids, which form via self-aggregated of cultured cells, are a kind of 3D model that demonstrates the interactions between cells, or between cells and the extracellular matrix. Therefore, the internal environment and physiological status, at least in part, can be recapitulated in the spheroids, making them a reliable tool for drug screening and functional studies [22–24]. Pingitore et al. constructed human multilineage spheroids with HepG2 and LX-2 cells, and proved that the spheroids can be considered as a model of liver steatosis and fibrosis [25]. Furthermore, Romualdo et al. used spheroids composed of C3A and LX-2 cells to investigate the impact of sorafenib on steatosis-induced fibrogenesis in NAFLD [26]. Therefore, constructing the NAFLD spheroid model and investigating the effect of fucoidan in this model is suitable and necessary, and will provide new evidence regarding the therapeutic application of fucoidan in NAFLD.

In this study, the spheroids were constructed by fusing HepG2 and LX-2 cells, and NAFLD spheroid model was induced by stimulation with free fatty acids (FFAs). The effect of fucoidan on FFA-induced lipid accumulation and oxidative stress was investigated in both spheroids and HepG2 cells, and the potential molecular mechanism was explored. Furthermore, the inhibitory effect of fucoidan on the FFA-induced inflammatory response was also investigated.

Materials and methods

Spheroid construction

HepG2 cells were cultured as the previous described [27]. The HepG2/LX-2 spheroids were generated as described by Pingitore et al. [25]. Briefly, HepG2 and LX-2 cells were fused at a ratio of 24:1 and placed into a 96-well round-bottomed ultra-low attachment plate at 2000 cells/well in Modified Eagle Medium (MEM) (Sperikon Life Science & Biotechnology Co., Ltd) supplemented with 10% FBS. The final volume was 200 μL/well. They were incubated at 37 °C in a humidified atmosphere of 5% CO_2 and grown for a total of 96 h. During the 96 h incubation period, 100 μl of medium was removed from each well and replaced with 100 μL preheated fresh medium every 24 h. The volume of spheroids was calculated using the following formula: $4/3\ \pi r^3$, where "r" stands for the mean of the long and short diameter of the spheroid divided by 2.

Oil red O staining and intracellular TG measurement

FFAs was generated as described by Zhang et al. [28]. Briefly, the palmitic acid and oleic acid were diluted with 1% fatty acid-free bovine serum albumin (BSA) and mixed as the molar mass ratio of 1:2. The FFAs was added to the complete medium and used as the fat-supplemented medium (final FFAs concentration was 0.5mM). HepG2 cells were stimulated with BSA or FFAs for 24 h,

and then stimulated with DMSO (1%v/v) or fucoidan at a dose of 1, 10, 50, or 100 μg/mL for 24 h. Intracellular lipid droplets were stained using an oil red O staining kit (Solarbio, China), and intracellular triglyceride (TG) content was detected using a TG assay kit (Nanjing Jiancheng Bioengineering Institute, China) according to the manufacturer's instructions [28]. For the spheroids, HepG2 and LX-2 cells were cultured for 48 h at a ratio of 24:1, stimulated with BSA or FFAs for 24 h, and then further stimulated with DMSO or fucoidan (100 μg/mL) for an additional 24 h. Intracellular lipid droplets and TG content were measured as above described.

Cell viability measurement

To explore the cytotoxicity of fucoidan, the CCK-8 assay was used. HepG2 cells were cultured in a 96-well plate with complete medium and stimulated with DMSO or fucoidan (1, 10, 50, 100 μg/mL) for 24 h. After that, CCK8 working solution (MedChemExpress, USA) was added into each well and incubated at 37 °C for 30 min. The absorbance at 450 nm was measured using spectrophotometer (Thermo, USA), and the rate of alive cells was calculated relative to controls (%). Furthermore, HepG2 cells were cultured in a 96-well plate with complete medium, stimulated with BSA or FFAs for 24 h, incubated with DMSO or fucoidan (1, 10, 50, 100 μg/ml) for 24 h, and then the cell viability was measured as described above. For spheroids, HepG2 and LX-2 cells were cultured for 48 h at a ratio of 24:1. Spheroids were then stimulated with BSA or FFAs for 24 h, followed by DMSO or fucoidan (100 μg/mL) for 24 h. After that, the total cellular adenosine triphosphate (ATP) of spheroids was tested by the Cell-Titer-Glo® 3D cell viability assay (Promega, USA) as described by Li et al. [29]. Briefly, single spheroids were transferred into a white 96-well assay plate (Corning, USA) with 50 μL PBS. Next, 50 μL of assay reagent was added to each well and samples were vigorously mixed to allow the reagent to penetrate the spheroids. Cells were incubated in the dark at room temperature for 20 min, the plate was placed in the SpectraMax i3 (Molecular Devices, USA) counter and luminescence was measured using the SoftMax Pro 6.3 software (San Jose, USA), and the rate of alive cells was calculated relative to controls (%).

Measurement of intracellular oxidative stress levels

The intracellular levels of glutathione (GSH), glutathione reductase (GR), and glutathione peroxidase (GPx) were measured using commercially purchased assay kits (Beyotime Institute of Biotechnology, China) described by Li et al. [29]. Briefly, HepG2 cells were stimulated with BSA or FFAs for 24 h, after which cells were stimulated with DMSO or fucoidan (100 μg/mL) for 24 h. For spheroids, HepG2 and LX-2 cells were cultured for 48 h at a ratio of 24:1, treated with BSA or FFAs for an additional 24 h, and then further stimulated with DMSO or fucoidan (100 μg/ml) for 24 h. After that, the HepG2 cells and spheroids were collected by centrifugation at 3000 rpm for 5 min. The collected cells and spheroids were homogenized in 100 μL of assay kit cell lysis buffer (for the GR assay), sample homogenization buffer (for the GPx assays) or protein-removal reagent (for the GSH assay). Subsequently, the homogenate was centrifuged at 10,000 rpm for 10 min, and GPx, GR and GSH levels in the supernatants were measured according to manufacturer's instructions. In addition, the protein concentration of the supernatant was measured using a BCA protein assay, and the final measurement of GPx, GR, and GSH was normalized to the protein content.

Measurement of intracellular ROS and MDA levels

Intracellular ROS levels were measured using a 2,7-dichlorofluorescein diacetate (DCFH-DA) probe (Elabscience, China). HepG2 cells and spheroids were treated in a 96-well black plate with FFAs or BSA, as described above, after which they were stimulated with DMSO or fucoidan (100 μg/mL) for 24 h. Cells and spheroids were then incubated with FBS-free medium containing 10 μM DCFH-DA at 37 °C for 45 min, after which the cells and spheroids were washed with PBS. The intracellular fluorescence intensity of the probe was determined using a microplate reader at an excitation wavelength of 488 nm and an emission wavelength of 525 nm.

The relative malondialdehyde (MDA) concentration in lysate was detected using an MDA assay kit (Elabscience, China), according to the manufacturer's instructions. Briefly, the reaction of the MDA in the sample with thiobarbituric acid (TBA) generated an MDA-TBA adduct. The absorbance of MDA was measured with a microplate spectrophotometer at 450 nm. In addition, the protein concentration of the sample lysates was measured using a BCA protein assay kit, and the final measurement was normalized to the protein concentration.

Transmission electron microscopy (TEM) and immunofluorescence

HepG2 and LX-2 cells were fused at a ratio of 24:1 ratio and cultured for 96 h to construct the spheroids. Spheroids were fixed with 5% glutaraldehyde and processed, then the specimens were examined using a JEOL 1011 transmission electron microscope (JEOL, Tokyo, Japan). HepG2 cells and spheroids were fixed with 4% paraformaldehyde and permeabilized with 0.5% Triton X-100, then the HepG2 cells and spheroids were incubated with primary and then secondary antibodies. After that, the nuclei was stained with 4′,6-Diamidino-2-phenylindole (DAPI). Images of HepG2 cells and spheroids were captured under a fluorescence microscope (Nikon, Japan).

Table 1 Sequences of primers used in this study

Primer	Forward (5′-3′)	Reverse (5′-3′)
Nrf2	AGCCCAGCACATCCAGTCAG	AAACGTAGCC-GAAGAAACCTCA
TNF-α	GCTGCACTTTGGAGTGATCG	GCTGCACTTTGGAGTGATCG
IL-6	GTAGTGAGGAACAAGC-CAGAGC	TACATTTGCCGAAGAGCCCT
β-actin	CATCCTCACCCTGAAGTACCCC	AGCCTGGATGCAACGTA-CATG

Table 2 Antibodies used in this study

Antibodies	Company	Catalog number
NQO1	Sangon Biotech	D161049
HO-1	Sangon Biotech	D220756
GCLC	Sangon Biotech	D123963
PI3K	Sangon Biotech	D262049
p-PI3K	Bioss	bs-6417R
AKT	HUABIO	ER62638
p-AKT	Santa Cruz Biotechnology	sc-514,032
Nrf2	Sangon Biotech	D121053
p-Nrf2	Sangon Biotech	D291025
KEAP1	Santa Cruz Biotechnology	sc-365,626
NF-κB	CST	8242T
p-NF-κB	Abcam	ab31624
GAPDH	Proteintech	10494-1-AP
Lamin B	HUABIO	R1508-1

Knockdown of Nrf2 with small hairpin RNA

Adenovirus with antisense of Nrf2 small hairpin RNA (shRNA) was obtained from Genechem (Shanghai, China). The sequence of shRNA for Nrf2 was as follows: 5′-CCGGCATTTCACTAAACACAA-3′. HepG2 cells were cultured in a 6-well plate, grown to 50–60% confluence and then transfected for 5 h with Nrf2 adenovirus at a multiplicity of infection of 100. Cells were then supplemented with fresh medium, and cultured continuously for an additional 48 h. After that, cells were harvested and the expression of Nrf2 was analyzed by quantitative real-time PCR (qRT-PCR) and western blotting to confirm the efficiency of Nrf2 knockdown.

Nuclear and cytoplasmic proteins extraction

Nuclear and cytoplasmic proteins were extracted as described by Li et al. [29]. Briefly, HepG2 cells and spheroids were treated with FFAs and fucoidan as described above, after which cells and spheroids were harvested by gentle scraping and centrifugation at 3000 rpm for 5 min. The nuclear and cytoplasmic proteins of HepG2 cells and spheroids were collected using a commercial assay kit (Sangon Biotech, China).

RNA extraction, qRT-PCR and Western blotting

Total RNA was extracted from HepG2 cells and spheroids using AG RNAex Pro Reagent (Accurate Biology, China). RNA was then transcribed into cDNA using PrimeScript RT reagent kit with a genomic DNA Eraser (Takara, Japan). Gene expression was quantified using qRT-PCR as described by Chu et al. [30]. The sequences of primers for qRT-PCR are listed in Table 1. Total protein extracted from HepG2 cells and spheroids and western blotting were conducted as described by Chu et al. [30]. Information regarding the primary antibodies is listed in Table 2.

Statistical analysis

Statistical analysis was performed using SPSS 17.0 software. All results were expressed as the mean ± standard deviation. Differences between the two groups were compared using the student's *t* test. Each experiment was independently performed at least three times. A P value of < 0.05 was considered statistically significant.

Results

Fucoidan decreased FFA-induced lipid accumulation in HepG2 cells and spheroids

The experimental flow of the NAFLD cell model construction and subsequent fucoidan treatment is shown in Fig. 1A. The cytotoxicity of fucoidan on HepG2 cells was evaluated by CCK8 assay, and the results showed that cell viability was not affected by different doses of fucoidan (1, 10, 50, 100 μg/mL) (Fig. 1B). As shown in Fig. 1C, FFA treatment reduced the viability of HepG2 cells compared to control, while fucoidan treatment at increasing doses (1, 10, 50, 100 μg/mL) significantly reversed the FFA-induced decline in HepG2 cell viability, with no difference of the cell viability between 1 vs. 100 μg/mL treatment dose. To assess the impact of fucoidan on lipid accumulation in HepG2 cells, oil red O staining was conducted and the intracellular TG content was measured. As the results showed in Fig. 1D, FFA treatment markedly increased intracellular TG content, but this could be reversed by fucoidan treatment. Oil red O staining indicated that fucoidan can inhibit intracellular lipid droplet formation effectively in a dose-dependent manner (Fig. 1E). According to the above results, the 100 μg/mL dose of fucoidan was used in the subsequent experiments.

The NAFLD spheroid model was constructed and the effect of fucoidan on lipid accumulation in spheroids was evaluated (Fig. 2A). HepG2 and LX-2 cells were cultured for 96 h at a 24:1 ratio, during which time cells gradually adhered to the circular 3D structure (Fig. 2B). TEM was used to measure the intracellular structure of the spheroids, and the results showed that spheroids possessed normal hepatocyte morphology (Fig. 2C). During the culturing of the spheroids, there was no significant difference in the volume of spheroids in the control group, the FFA + DMSO group, and the FFA + fucoidan group (Fig. 2D). The cell viability of the spheroids was evaluated by measuring the ATP levels of spheroids. FFA

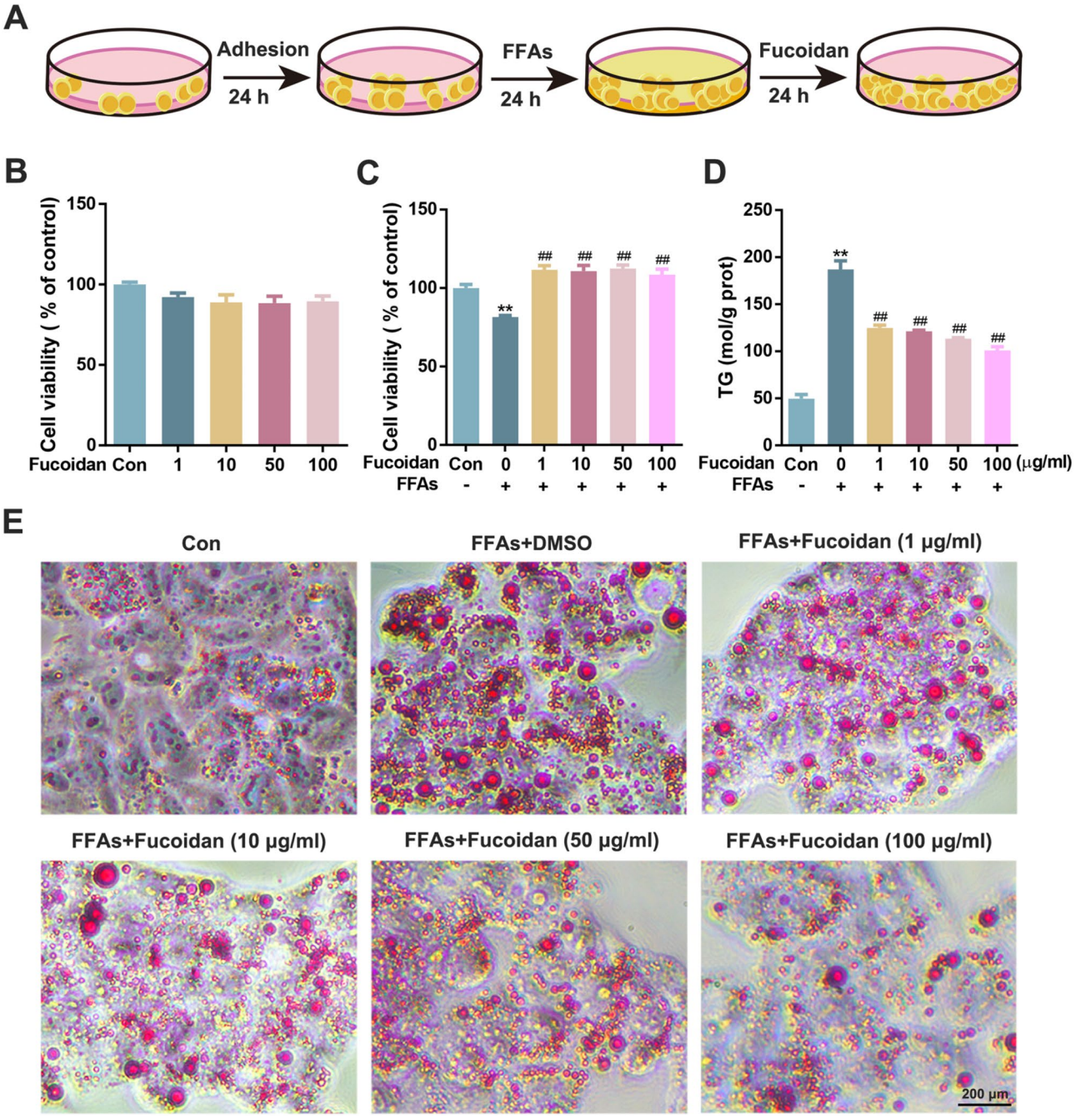

Fig. 1 Fucoidan reduced FFA-induced lipid accumulation in HepG2 cells. (**A**) The experimental flow of FFAs stimulation and fucoidan treatment in HepG2 cells. HepG2 cells were adhered in plates and cultured for 24 h, then stimulated with FFA (0.5 mM) for 24 h, further treated with DMSO (control) or fucoidan (1, 10, 50, 100 μg/ml) for additional 24 h. (**B**) Detection of fucoidan cytotoxicity in HepG2 cells. HepG2 cells were stimulated with DMSO or fucoidan (1, 10, 50, 100 μg/ml) for 24 h, then the cell viability was detected using the CCK-8 assay. (**C**) Fucoidan improved FFA-induced cytotoxicity. HepG2 cells were treated as described in (**A**), and then the cell viability was detected using the CCK-8 assay. (**D**) Fucoidan decreased intracellular TG content in HepG2 cells. HepG2 cells were treated as described in (**A**), and then the intracellular TG content was measured. (**E**) Fucoidan inhibited lipid droplet formation in HepG2 cells. HepG2 cells were treated as described in (**A**), and then the cells were stained with oil red O. Data were analyzed by the student's t test and expressed as the mean ± SD ($n = 3$). * represents the differences compared to the control group. # represents the differences compared to the DMSO group. ** $P < 0.01$; ## $P < 0.01$

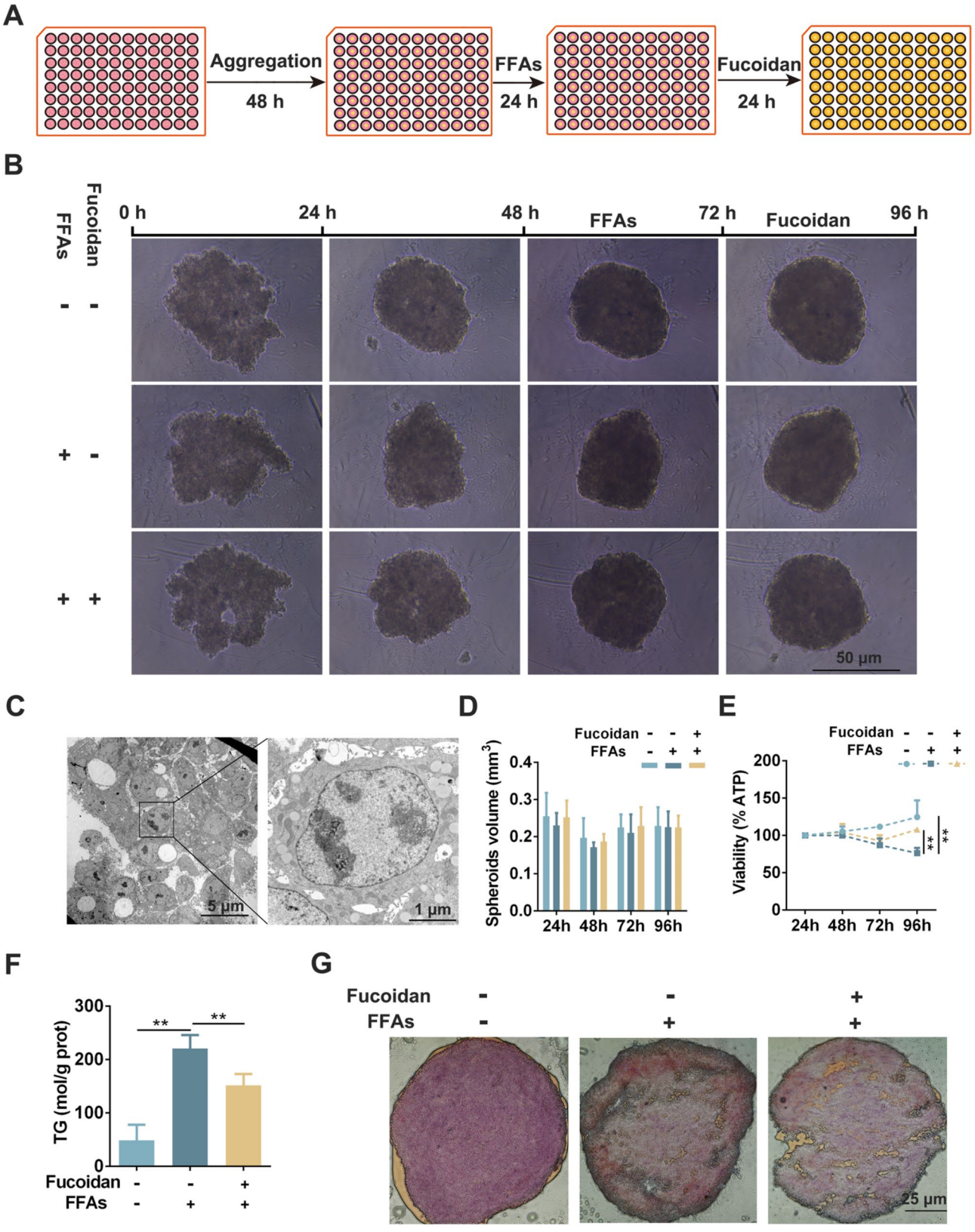

Fig. 2 (See legend on next page.)

(See figure on previous page.)

Fig. 2 Fucoidan reduced FFA-induced lipid accumulation in spheroids. (**A**) The experimental flow of FFAs stimulation and fucoidan treatment in spheroids. Spheroids were aggregated for 48 h, then stimulated with FFAs (0.5 mM) for 24 h, further treatment with DMSO (control) or fucoidan (100 μg/ml) for additional 24 h. (**B**) The morphology of spheroids during the experimental flow as described in (**A**). (**C**) Intracellular morphology of spheroids. HepG2 and LX-2cells were fused at a ratio of 24:1 ratio and cultured for 96 h to construct the spheroids, then the spheroids were subjected to the TEM detection. (**D**) The volume of spheroids during the experimental flow as described in (**A**). (**E**) Fucoidan improved FFA-induced cytotoxicity. Spheroids were treated as described in (**A**), and then the viability of spheroids was detected using the CCK-8 assay. (**F**) Fucoidan decreased the intracellular TG content in spheroids. Spheroids were treated as described in (**A**), and then the intracellular TG content was measured. (**G**) Fucoidan inhibited lipid droplet formation in spheroids. Spheroids were treated as described in (**A**), and then the Spheroids were stained with oil red O. Data were analyzed by student's t test and expressed as the mean ± SD ($n = 3$). * represents the differences between the two groups. ** $P < 0.01$

stimulation significantly inhibited the viability of spheroids after 96 h culture, which was measured by normalizing ATP levels to spheroid volume. However, fucoidan treatment significantly reversed the reduction in the viability of spheroids after 96 h culture (Fig. 2E). Similarly, in HepG2 cells, FFA stimulation remarkably elevated the intracellular TG content of spheroids, while fucoidan treatment significantly alleviated the increase in intracellular TG content of spheroids (Fig. 2F). Oil red O staining further verified that fucoidan could inhibit FFA-induced lipid accumulation in spheroids (Fig. 2G). These results indicated that fucoidan can ameliorate FFA-induced lipid accumulation in HepG2 cells and spheroids.

Fucoidan inhibited FFA-induced oxidative stress in HepG2 cells and spheroids

To explore the effect of fucoidan on FFA-induced oxidative stress in HepG2 cells and spheroids, the intracellular levels of ROS, MDA, GSH, GR, and GPx, and the expression of antioxidant genes NQO1, GCLC, and HO-1 were measured. FFA treatment markedly increased intracellular levels of ROS and MDA, and decreased intracellular levels of GSH, GR, and GPx in HepG2 cells. After 24 h treatment of fucoidan, the intracellular levels of ROS and MDA were decreased, and levels of GSH, GR, and GPx were elevated (Fig. 3A and E). Similarly, after treatment of spheroids with fucoidan, the FFA-induced elevation of intracellular ROS and MDA was reversed, as was the FFA-induced decline in intracellular levels of GSH, GR, and GPx (Fig. 3I and M). Furthermore, FFA stimulation inhibited the protein expression of NQO1, GCLC, and HO-1, however subsequent fucoidan treatment reversed this effect in HepG2 cells and spheroids (Fig. 3F, H, N and P). These results proved that fucoidan can undo FFA-induced oxidative stress in HepG2 cells and spheroids.

Fucoidan activates the PI3K/AKT/Nrf2 signaling pathway

Previous researches have reported that the PI3K/AKT pathway is involved in the regulation of metabolic functions by fucoidan [17], and that the PI3K/AKT/Nrf2 pathway is participated in antioxidant effects as phosphorylated Nrf2 can enter the nucleus to activate the transcription of antioxidant genes [29]. To explore the possible mechanism that is participated in the antioxidant response of fucoidan, the activation of the PI3K/AKT/Nrf2 pathway was measured. As shown in Fig. 4A and B, FFA stimulation inhibited the activity of PI3K/AKT, by decreasing the phosphorylation of PI3K and AKT, however, fucoidan treatment markedly promoted PI3K and AKT phosphorylation in HepG2 cells. In addition, fucoidan treatment markedly enhanced the expression and phosphorylation of Nrf2, which was inhibited by FFAs stimulation (Fig. 4C). Furthermore, fucoidan treatment induced the translocation of Nrf2 from the cytoplasm to the nucleus in the presence of FFAs in HepG2 cells (Fig. 4D and E).

To further validate the key role of Nrf2 in the molecular mechanism of fucoidan, Nrf2-shRNA was stably transfected into HepG2 cells, and the cells were fused with LX-2 cells to form spheroids. qRT-PCR and western blotting showed that Nrf2 was successfully knocked down in HepG2 cells and spheroids (Fig. 4F and G). In spheroids, fucoidan treatment could not elevate Nrf2 expression after FFA stimulation when Nrf2 was knocked down (Fig. 4H). The above results suggest that fucoidan activates the PI3K/AKT/Nrf2 pathway.

Fucoidan inhibited FFA-induced lipid accumulation and oxidative stress by activating the PI3K/AKT/Nrf2 pathway

To determine whether the PI3K/AKT/Nrf2 pathway was involved in fucoidan-mediated protection against FFA-induced lipid accumulation and oxidative stress, intracellular TG content and oxidative stress levels were measured in HepG2 cells and spheroids after Nrf2 knock down. As shown in Fig. 5A and G, Nrf2 knock-down remarkably abolished the protective effect of fucoidan on FFA-induced lipid accumulation in HepG2 cells and spheroids. In addition, Nrf2 knock-down can markedly abolish the amelioration of FFA-induced oxidative stress after treatment with fucoidan in HepG2 cells and spheroids (Fig. 5B, F, H and L). Furthermore, Nrf2 knock-down can markedly reverse the up-regulation of NQO1, GCLC and HO-1 after treatment with fucoidan in the presence of FFAs in HepG2 cells and spheroids (Fig. 5M and R). These results indicate that fucoidan can inhibit FFA-induced lipid accumulation and oxidative stress by activating the Nrf2 signaling pathway in HepG2 cells and spheroids.

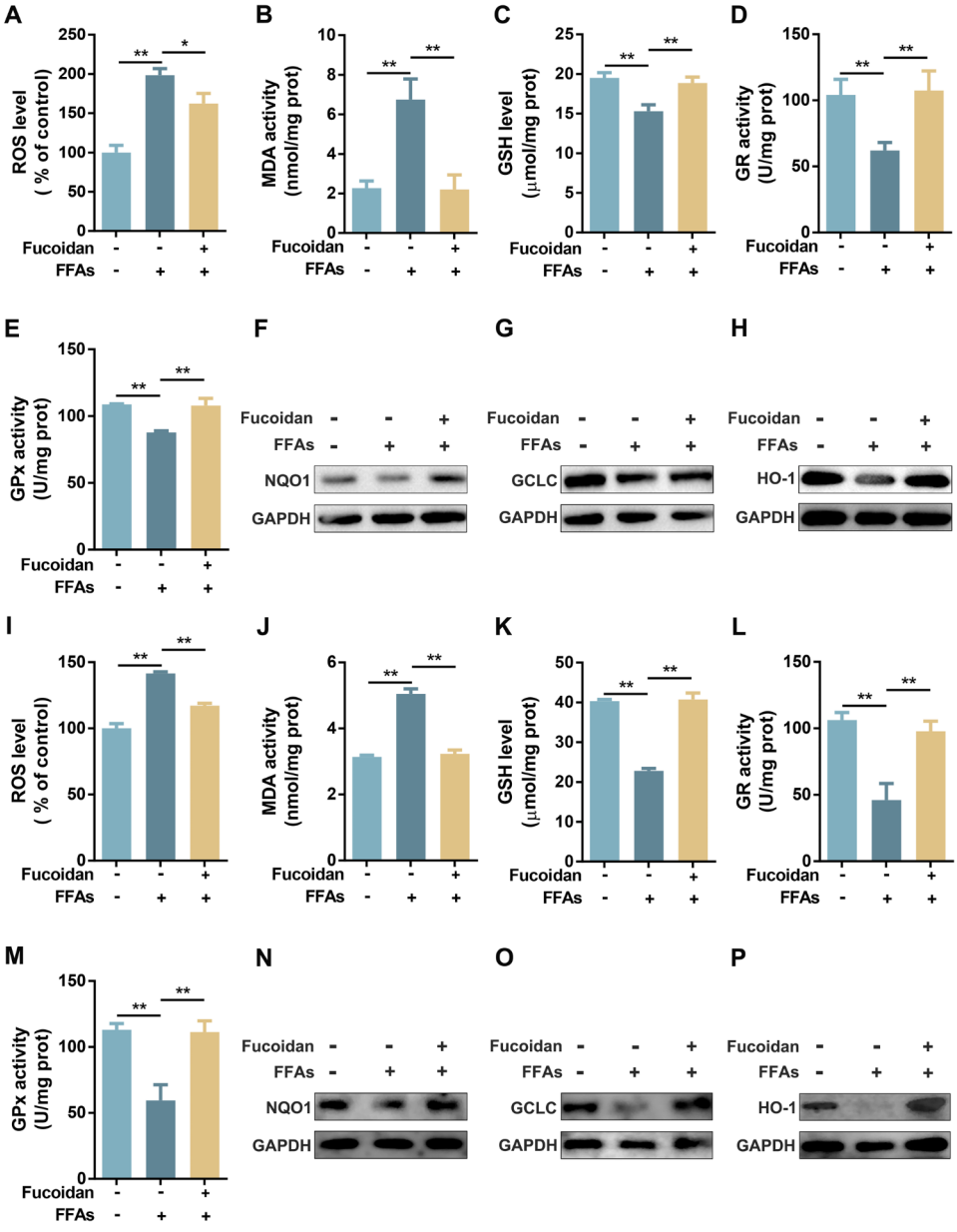

Fig. 3 Fucoidan alleviates FFA-induced oxidative stress in HepG2 cells and spheroids. (**A**-**E**) Fucoidan inhibits FFA-induced oxidative stress in HepG2 cells. HepG2 cells were stimulated with FFAs (0.5 mM) for 24 h, further treatment with DMSO (control) or fucoidan (100 μg/ml) for additional 24 h. The intracellular levels of ROS, MDA, GSH, GR, and GPx were measured. (**F**-**H**) Fucoidan inhibits the expression of antioxidant factors in HepG2 cells. HepG2 cells were treated as described in (**A**-**E**), and then the expression of NQO1, GCLC, and HO-1 were measured by western blotting. (**I**-**M**) Fucoidan inhibits FFA-induced oxidative stress in spheroids. Spheroids were aggregated for 48 h, then stimulated with FFAs (0.5 mM) for 24 h, further treatment with DMSO (control) or fucoidan (100 μg/ml) for additional 24 h. The intracellular levels of ROS, MDA, GSH, GR, and GPx were measured. (**N**-**P**) Fucoidan inhibits the expression of antioxidant factors in spheroids. Spheroids were treated as described in (**I**-**M**), and then the expression of NQO1, GCLC, and HO-1 were measured by western blotting. Data were analyzed by student's t test and expressed as the mean ± SD ($n = 3$). * represents the differences between the two groups. * $P < 0.05$; ** $P < 0.01$

Fucoidan inhibited FFA-induced inflammation by activating the Nrf2 signaling pathway

Previous researches have suggested that excess production of ROS possesses the pro-inflammatory effect during the progression of NAFLD [9, 10]. First, the intervention effect of fucoidan on FFA-induced inflammatory responses was investigated in HepG2 cells. FFA stimulation up-regulated the expression of TNF-α and IL-6, while fucoidan significantly reversed the up-regulation of TNF-α and IL-6 (Fig. 6A and B). Furthermore, FFA treatment led to increased phosphorylation and nuclear translocation of P65 NF-κB, while fucoidan significantly inhibited both of these effects (Fig. 6C and E).

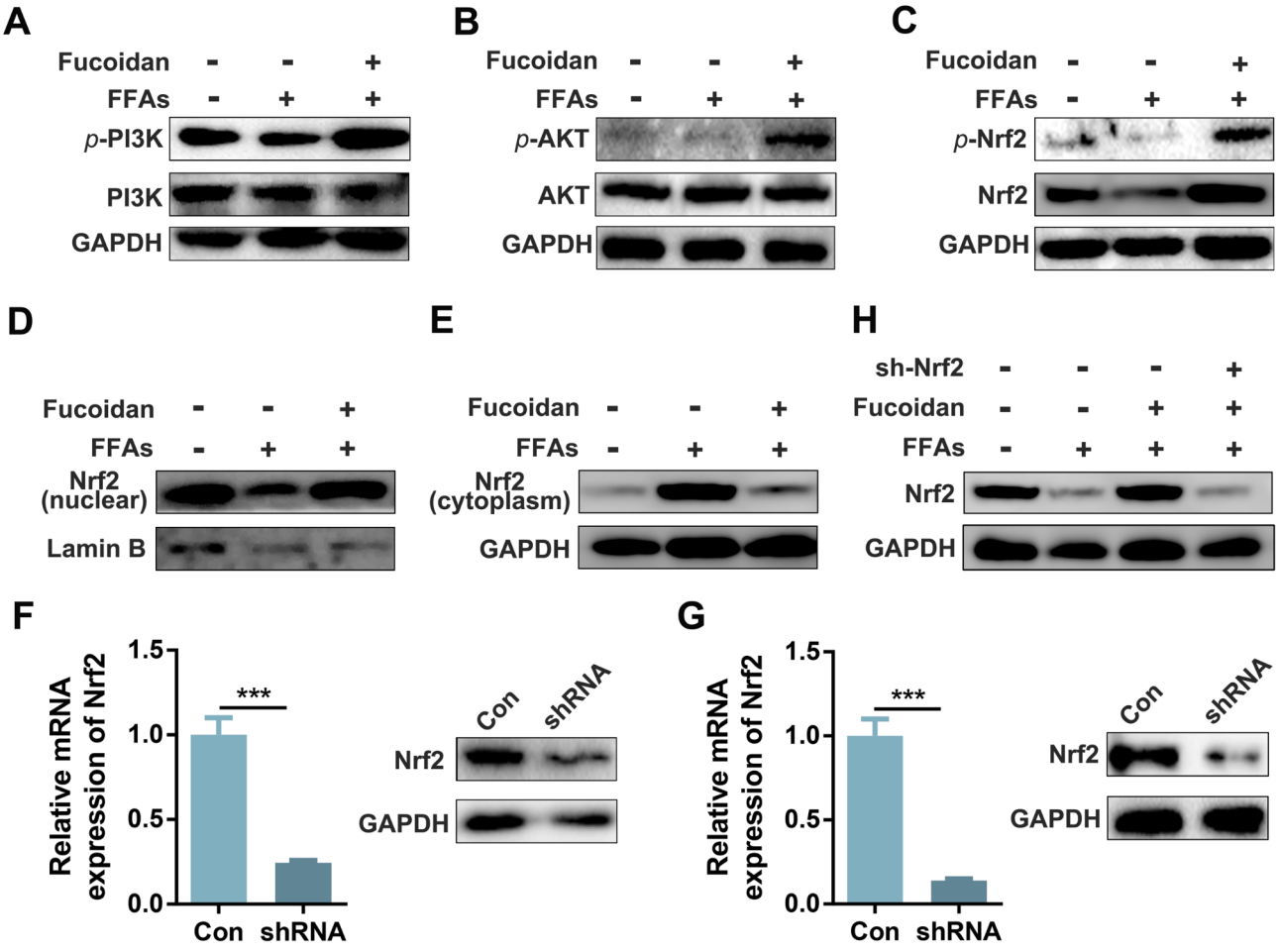

Fig. 4 Fucoidan activates the PI3K/AKT/Nrf2 signaling pathway. (**A**-**B**) Fucoidan promotes the phosphorylation of PI3K and AKT. HepG2 cells were stimulated with FFAs (0.5 mM) for 24 h, further treatment with DMSO (control) or fucoidan (100 μg/ml) for additional 24 h. The phosphorylation levels of PI3K and AKT were analyzed by western blotting. (**C**) Fucoidan increases the expression and phosphorylation of Nrf2. HepG2 cells were treated as described in (**A**-**B**), and the expression and phosphorylation of Nrf2 were analyzed by western blotting. (**D**-**E**) Fucoidan promotes the nuclear translocation of Nrf2. HepG2 cells were treated as described in (**A**-**B**), and the protein levels of Nrf2 in nuclear and cytoplasm were measured by western blotting. (**F**-**G**) Nrf2 knock-down in HepG2 cells and spheroids. HepG2 cells were transfected with Adenovirus contains antisense of Nrf2 shRNA for 5 h, then supplemented with fresh medium, and continuously cultured for an additional 48 h. Spheroids were constructed with Adenovirus transfected HepG2 cells. The expression of Nrf2 in HepG2 cells and spheroids were analyzed by qRT-PCR and western blotting. (**H**) Nrf2 shRNA abolished the overexpression of Nrf2 induced by Fucoidan in spheroids. Spheroids were aggregated with Adenovirus transfected HepG2 cells for 48 h, then stimulated with FFAs (0.5 mM) for 24 h, further treatment with DMSO (control) or fucoidan (100 μg/ml) for additional 24 h. The expression of Nrf2 in spheroids was analyzed by western blotting. Data were analyzed by student's t test and expressed as the mean ± SD ($n = 3$). * represents the differences between the two groups. *** $P < 0.001$

These results were further confirmed by immunofluorescence staining (Fig. 6F).

To explore whether Nrf2-mediated antioxidant processes are participated in fucoidan-mediated protection against FFA-induced inflammation, Nrf2 was knocked down in the HepG2 cells by shRNA, and cells were fused with LX-2 cells to form spheroids. Spheroids were treated with FFAs followed by fucoidan. Nrf2 knock-down significantly elevated the expression of TNF-α and IL-6 (Fig. 6G and H). Meanwhile, Nrf2 knock-down inhibited the reduction in P65 NF-κB phosphorylation and nuclear translocation induced by fucoidan (Fig. 6I and K). Furthermore, the above results were also validated by immunofluorescence staining (Supplementary Fig. 1). These results indicate that fucoidan can trigger the Nrf2-mediated antioxidant process, inhibit the overproduction of ROS, and lead to reduced P65 NF-κB activation, thereby partially inhibiting the FFA-induced inflammatory response.

Discussion

The pathogenesis and therapy of NAFLD have been the focus of global attention. Lipid accumulation, hepatic steatosis, and oxidative stress are the key characteristics of NAFLD [31]. Therefore, inhibition of lipid accumulation and reduction of oxidative stress are beneficial to the prevention and treatment of NAFLD. Spheroids have been a reliable tool for drug screening and for functional

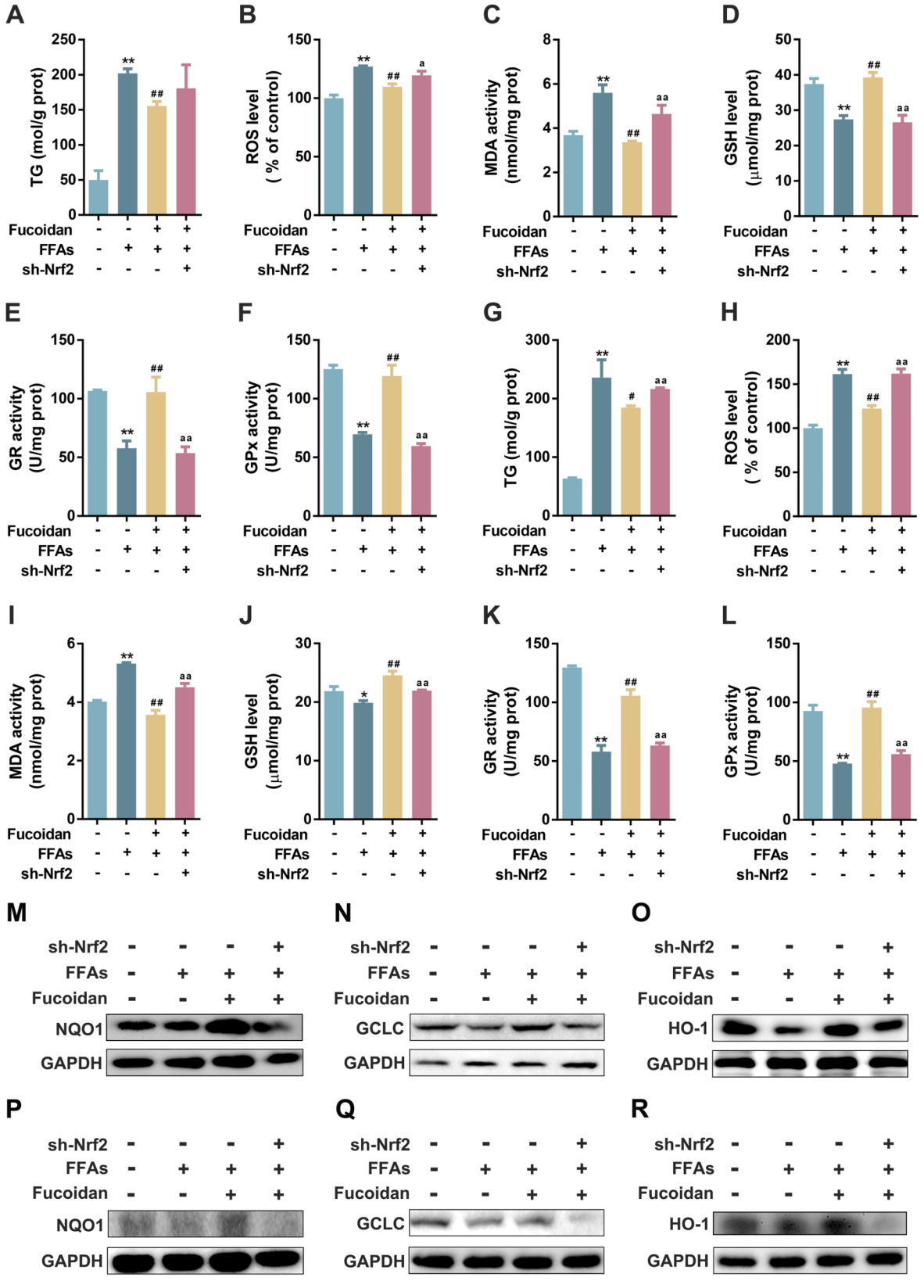

Fig. 5 (See legend on next page.)

(See figure on previous page.)

Fig. 5 Fucoidan alleviates FFA-induced lipid accumulation and oxidative stress via the Nrf2 signaling pathway. (**A**) Nrf2 knock-down inhibits the reduction in intracellular TG content by fucoidan in HepG2 cells. HepG2 cells with Nrf2 knocked down were stimulated with FFAs (0.5 mM) for 24 h, further treatment with DMSO (control) or fucoidan (100 μg/ml) for additional 24 h. And then the intracellular TG content was measured. (**B**-**F**) Nrf2 knock-down inhibits the remission of oxidative stress by fucoidan in HepG2 cells. HepG2 cells with Nrf2 knocked down were treated as described in (**A**), and the intracellular levels of ROS, MDA, GSH, GR, and GPx were measured. (**G**) Nrf2 knock-down inhibits the reduction of intracellular TG content by fucoidan in spheroids. Spheroids with Nrf2 knocked down were stimulated with FFAs (0.5 mM) for 24 h, further treatment with DMSO (control) or fucoidan (100 μg/ml) for additional 24 h. And then the intracellular TG content was measured. (**H**-**L**) Nrf2 knock-down inhibits the remission of oxidative stress by fucoidan treatment in spheroids. Spheroids with Nrf2 knocked down were treated as described in (**G**), and the intracellular levels of ROS, MDA, GSH, GR, and GPx were measured. (**M**-**O**) Nrf2 knock-down inhibits the reduction of antioxidant factor expression by fucoidan in HepG2 cells. HepG2 cells with Nrf2 knocked down were treated as described in (**A**), and the expression of NQO1, GCLC, and HO-1 were assayed by western blotting. (**P**-**R**) Nrf2 knock-down inhibits the reduction of antioxidant factor expression by fucoidan in spheroids. Spheroids with Nrf2 knocked down were treated as described in (**G**), and the expression of NQO1, GCLC, and HO-1 were assayed by western blotting. Data were analyzed by student's t test and expressed as the mean ± SD ($n = 3$). * represents the differences compared to control group. $^{\#}$ represents the differences compared to the DMSO group. ^{a} represents the differences compared to the FFA group. * $P < 0.05$; ** $P < 0.01$; $^{\#}P < 0.05$; $^{\#\#}P < 0.01$; $^{a}P < 0.05$; $^{aa}P < 0.01$

study due to their somewhat analogous internal environment and physiological status [23, 24]. This study systematically investigated the protective effect of fucoidan on FFA-induced lipid accumulation and oxidative stress, and the potential molecular mechanism in NAFLD spheroids and HepG2 cell. We found that fucoidan can reduce FFA-induced lipid accumulation, ROS overproduction and oxidative stress by activating the PI3K/AKT/Nrf2 pathway. In addition, fucoidan also restrained FFA-induced activation of NF-κB and inhibited the expression of its downstream inflammatory factors via the Nrf2 signaling pathway. This is the first study to directly use spheroids as in vitro model of NAFLD to demonstrate the impact of fucoidan on the amelioration of NAFLD, and our results have provided new evidence regarding the molecular mechanism involved in the protective effect of fucoidan against NAFLD.

The development of NAFLD requires the retention of high levels of lipids in hepatocytes [32]. Hepatocellular lipids overload associated with increased liver TG content can lead to hepatocyte steatosis and lipid toxicity [33]. This study found that FFA exposure elevated the lipid content within spheroids and HepG2 cells. Oxidative stress is recognized as an important factor contributing to the progression of NAFLD, while excessive ROS accumulation is the main cause of mitochondrial dysfunction, hepatocyte injury, inflammatory response, and fibrosis in the pathogenesis of NAFLD. Therefore, focusing on the inhibition of hepatic oxidative stress is conducive to treat NAFLD [34–36]. Many studies have shown that sulfated polysaccharides can ameliorate hepatic oxidative stress by activating the antioxidant proteins [37]. Fucoidan is a kind of sulfated polysaccharide and possesses a variety of anti-oxidative, anti-inflammatory, lipid-lowering and liver protective functions [17–19]. In previous in vivo studies, fucoidan was shown to inhibit HFD-induced hepatic TG accumulation and suppress oxidative stress in a NAFLD rat model [38]. The results in this in vitro study showed that fucoidan can markedly inhibit FFA-induced lipid accumulation in spheroids and HepG2 cells, which verified the lipid-lowering effect of fucoidan in NAFLD spheroids and cell models. Furthermore, fucoidan also exhibited an excellent antioxidant effect in spheroids and HepG2 cells. Treatment with fucoidan can improve the activities of GSH, GR and GPx, increase the expression of antioxidant factors NQO1, GCLC and HO-1, and inhibit the overproduction of ROS and MDA, therefore alleviating liver cell damage. These findings demonstrated that fucoidan could act a protective role in NAFLD by improving hepatic oxidative stress.

Accumulated studies have shown that fucoidan may be involved in regulating the PI3K/AKT pathway, MAPK pathway, and caspase pathway [17, 39, 40]. Activation of PI3K/AKT can enhance the activity of Nrf2, enhance the antioxidant capacity of liver cells, and alleviate mitochondrial dysfunction [41]. Nrf2 is a regulator of cell resistance to active oxidants and a key transcription factor regulating the expression of various cell protective genes (GSH, GR NQO1, HO-1, etc.) [42–44]. Deng et al. report that fucoidan can promote macrophages glycolysis and regulate M1 macrophages differentiation by activating PI3K/AKT/mTOR pathway [45]. Shiau et al. summarized the physiology of fucoidan-modulated metabolism and concluded that fucoidan may modulate oxidative stress and PI3K/AKT/mTOR signaling pathway to implement metabolic regulation [46]. In this study, our results showed that fucoidan treatment up-regulated the PI3K and AKT phosphorylation, and increased the expression and phosphorylation of Nrf2, thereby promoting the translocation of Nrf2 to the nucleus. When Nrf2 expression was knocked down, the lipid-lowering and anti-oxidative effects of fucoidan were partially abolished in spheroids and HepG2 cells. These results demonstrate that fucoidan exerted antioxidant effects by activating the PI3K/AKT/Nrf2 pathway. Interestingly, previous researches have reported that fucoidan can activate the PI3K/AKT pathway in colon cancer and breast cancer [45, 47], but inhibit the activation of PI3K/AKT in several metabolic diseases in rats [46, 48]. This contradiction may suggest that fucoidan exerts different roles depending on the specific cellular environment or conditions,

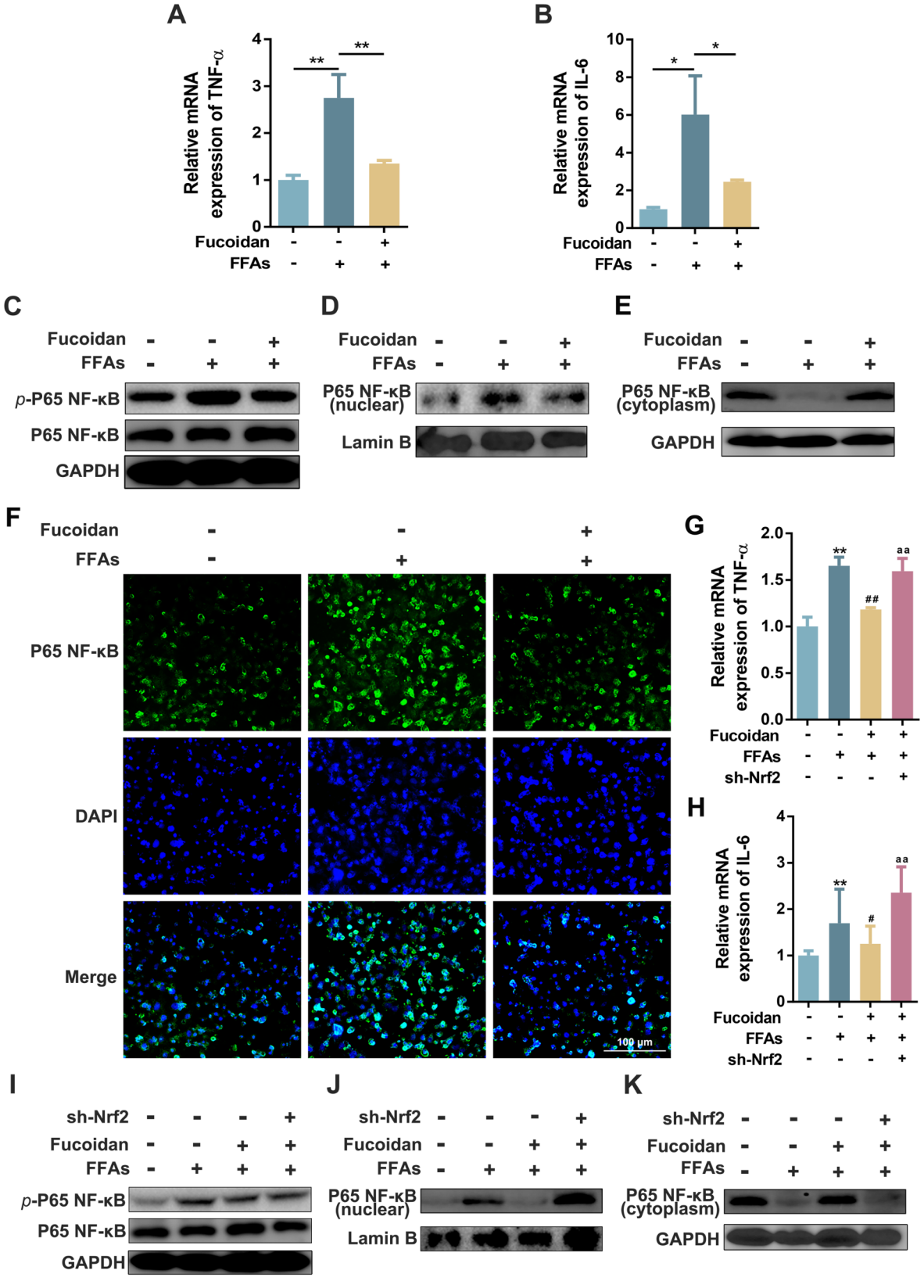

Fig. 6 (See legend on next page.)

(See figure on previous page.)

Fig. 6 Fucoidan inhibits FFA-induced inflammatory responses through the Nrf2 signaling pathway. (**A**-**B**) Fucoidan decreased the expression of inflammatory factors induced by FFAs in HepG2 cells. HepG2 cells were stimulated with FFAs (0.5 mM) for 24 h, further treatment with DMSO (control) or fucoidan (100 μg/ml) for additional 24 h. The expression of TNF-α and IL-6 were measured by qRT-PCR. (**C**) Fucoidan inhibited the phosphorylation of P65 NF-κB induced by FFAs in HepG2 cells. HepG2 cells were treated as described in (**A**-**B**), and the phosphorylation of P65 NF-κB were assayed by western blotting. (**D**-**F**) Fucoidan inhibited nuclear translocation of P65 NF-κB induced by FFAs in HepG2 cells. HepG2 cells were treated as described in (**A**-**B**), and the nuclear translocation of P65 NF-κB were assayed by western blotting and Immunofluorescence assay. (**G**-**H**) Nrf2 knock-down abolished the effect of fucoidan on the expression of inflammatory factors in spheroids. Spheroids with Nrf2 knocked down were stimulated with FFAs (0.5 mM) for 24 h, further treatment with DMSO (control) or fucoidan (100 μg/ml) for additional 24 h. The expression of TNF-α and IL-6 were measured by qRT-PCR. (I-K) Nrf2 knock-down inhibited the reduction of phosphorylation and nuclear translocation of P65 NF-κB by fucoidan in spheroids. Spheroids with Nrf2 knocked down were treated as described in (**G**-**H**), and the phosphorylation and nuclear translocation of P65 NF-κB were assayed by western blotting. Data were analyzed by student's t test and expressed as the mean ± SD ($n = 3$). * represents the differences the two groups or compared to control group. # represents the differences compared to the DMSO group. a represents the differences compared to the FFA group. * $P < 0.05$; ** $P < 0.01$; # $P < 0.05$; ## $P < 0.01$; aa $P < 0.01$

which implies that a more comprehensive understanding of its role in different biological contexts is required.

According to the 'multiple-hit' hypothesis of the pathogenesis of NAFLD, excessive accumulation of TG, "toxic" levels of serum FFAs and free cholesterol can cause oxidative stress and ROS production and endoplasmic reticulum stress, altogether lead to hepatic inflammation and the progression of NAFLD [8]. Reduction of antioxidant defenses can further aggravate the inflammatory response in the liver [49]. NF-κB proteins are a class of transcription factors critical in inflammation [50]. In the context of oxidative stress, increased levels of ROS in hepatocytes can activate the transcription of NF-κB, subsequently, P65 NF-κB can then further regulate the expression of IL-6 and TNF-α [51]. Therefore, reducing ROS overproduction in the liver is essential to inhibit P65 NF-κB-mediated inflammation. Nrf2 inhibits the progression of NAFLD to NASH by regulating the inflammatory cell recruitment and antioxidant responses to counteract the pro-inflammatory process [52]. Previous researches proved that PI3K/AKT can affect the NF-κB signaling pathway [53]. Therefore, fucoidan may inhibit FFA-induced liver inflammation by triggering an Nrf2-activated antioxidant cascade. In this study, fucoidan reduced FFA-induced ROS overproduction in spheroids by the PI3K/AKT/Nrf2 pathway, and also markedly reduced the levels of TNF-α and IL-6. Furthermore, Nrf2 knock-down significantly elevated the expression of TNF-α and IL-6, and inhibited the reduction of P65 NF-κB phosphorylation and nuclear transport induced by fucoidan. Therefore, fucoidan can inhibit FFA-induced activation of P65 NF-κB by the Nrf2 signaling pathway in spheroids. These results demonstrated that fucoidan can inhibit the ROS-induced inflammatory response via the PI3K/AKT/Nrf2 signaling pathway.

There were several limitations to this study. Firstly, only HepG2 cells were used to establish the spheroids and explore the function of fucoidan on FFA-induced lipid accumulation and the potential molecular mechanism, however, studies containing multiple hepatoma cell lines would be more logical. Secondly, although the HepG2-LX-2 spheroid model used in this study provides valuable insights, it lacks immune and endothelial cells, which are critical components of liver physiology. Thirdly, organoids can stimulate the physical environment more realistically than spheroids, therefore, organoids could be used in future studies to explore the impact of fucoidan on FFA-induced lipid accumulation and its potential molecular mechanism.

Conclusions

In summary, this study investigated the effects of fucoidan on FFA-induced lipid accumulation, oxidative stress, and inflammatory responses in NAFLD spheroid and HepG2 cells model. These fingings demonstrated that fucoidan can inhibit lipid accumulation and oxidative stress induced by FFAs through the PI3K/AKT/Nrf2 pathway. Furthermore, fucoidan can restrain the ROS-induced inflammatory response via the Nrf2 signaling pathway (Fig. 7). These results generated using the NAFLD spheroid and HepG2 cells model, can provide new evidence for the clinical use of fucoidan in the treatment of NAFLD and its potential molecular mechanism. In addition, these results also point out the significance of developing functional foods or nutraceuticals targeting NAFLD, and enhance the relevance of the study to both the scientific community and industry.

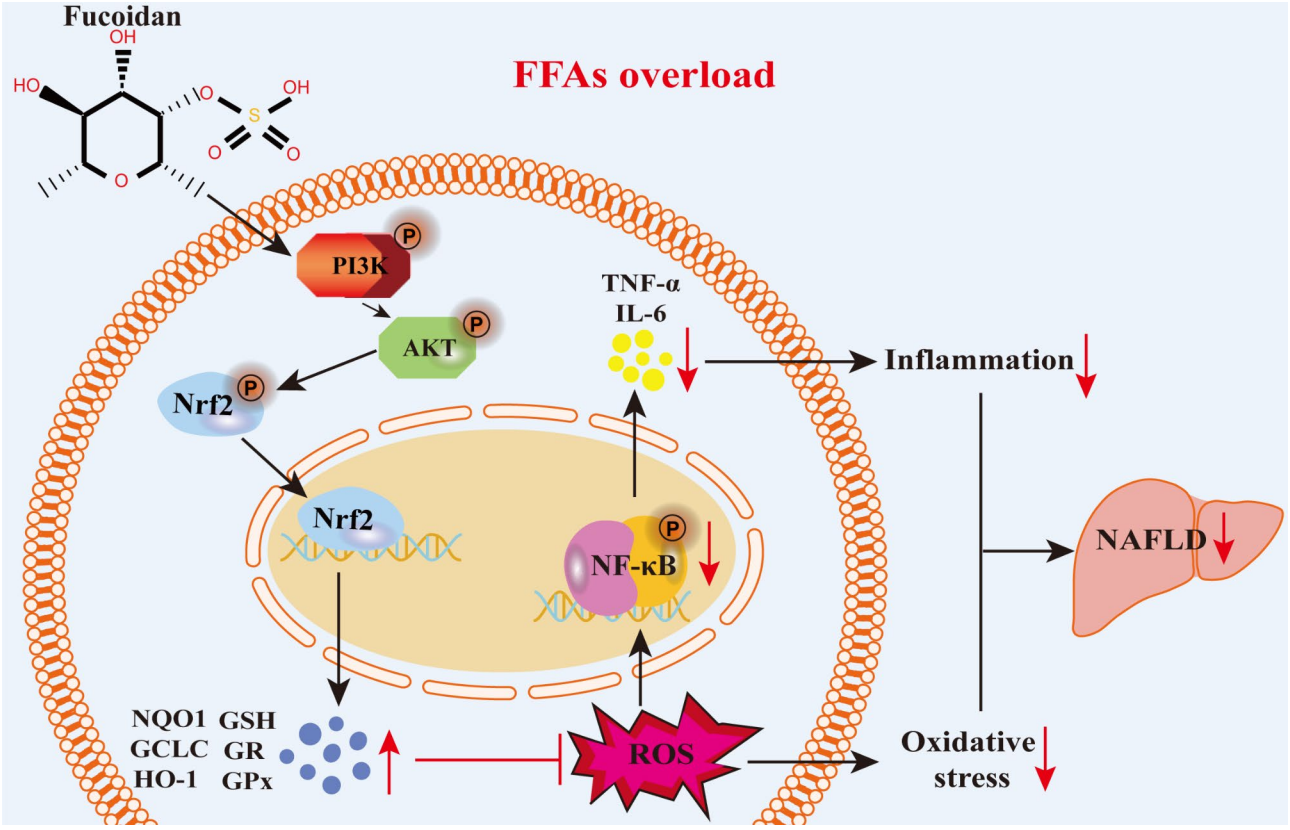

Fig. 7 Schematic representation of the possible mechanism by which fucoidan ameliorates FFA-induced oxidative stress and inflammation via regulation of the PI3K/AKT/Nrf2 signaling pathway in a NAFLD spheroid model

Abbreviations

3D	Three-dimensional
DAPI	4′,6-Diamidino-2-phenylindole
DCFH-DA	Dichlorofluorescein diacetate
DMEM	Dulbecco's Modified Eagle Medium
FBS	Fetal bovine serum
FFAs	Free fatty acids
GPx	Glutathione peroxidase
GR	Gluathione reductase
GSH	Glutathione
HFD	High-fat diet
IL-6	Interleukin-6
MDA	Malondialdehyde
MEM	Modified Eagle Medium
NAFLD	Non-alcoholic fatty liver disease
NASH	Non-alcoholic steatohepatitis
NF-κB	Nuclear factor kappa-B
qRT-PCR	Quantitative real-time PCR
ROS	Reactive oxide species
shRNA	Small hairpin RNA
TBA	Thiobarbituric acid
TG	Triglyceride
TNF-α	Tumor necrosis factor-α

Supplementary Information

The online version contains supplementary material available at https://doi.org/10.1186/s12944-025-02483-z.

Supplementary Material 1

Supplementary Material 2

Acknowledgements
We thank Medjaden Inc. for scientific editing and proofreading of this manuscript.

Author contributions
Conceptualization: Shousheng Liu and Yongning Xin; methodology, Xueru Chu, Xuan Wang, and Keqing Feng; software, Xueru Chu and Yanzhen Bi; resources, Shousheng Liu, Yongning Xin, and Yanzhen Bi; data curation, Xueru Chu and Xuan Wang; writing—original draft preparation, Xueru Chu, Xuan Wang, and Keqing Feng; writing—review and editing, Shousheng Liu and Yongning Xin; visualization, Keqing Feng; supervision, Shousheng Liu and Yongning Xin; project administration, Shousheng Liu and Yongning Xin. All authors have read and agreed to the published version of the manuscript.

Funding
This study was supported by Grants of National Natural Science Foundation of China (32171277, 82202416) and Natural Science Foundation of Shandong Province (ZR2022QH104).

Data availability
All data generated or analyzed in this study are available from the corresponding author for the reasonable request.

Declarations

Consent for publication
Not applicable.

Competing interests
The authors declare no competing interests.

Received: 9 January 2025 / Accepted: 12 February 2025

Published online: 17 February 2025

References

1. Le MH, Le DM, Baez TC, Wu Y, Ito T, Lee EY, Lee K, Stave CD, Henry L, Barnett SD, et al. Global incidence of non-alcoholic fatty liver disease: a systematic review and meta-analysis of 63 studies and 1,201,807 persons. J Hepatol. 2023;79:287–95.
2. Matchett KP, Paris J, Teichmann SA, Henderson NC. Spatial genomics: mapping human steatotic liver disease. Nat Reviews Gastroenterol Hepatol. 2024;21:646–60.
3. Quek J, Chan KE, Wong ZY, Tan C, Tan B, Lim WH, Tan DJH, Tang ASP, Tay P, Xiao J, et al. Global prevalence of non-alcoholic fatty liver disease and non-alcoholic steatohepatitis in the overweight and obese population: a systematic review and meta-analysis. Lancet Gastroenterol Hepatol. 2023;8:20–30.
4. Stefan N, Schick F, Birkenfeld AL, Häring H-U, White MF. The role of hepatokines in NAFLD. Cell Metabol. 2023;35:236–52.
5. Mantovani A, Petracca G, Beatrice G, Tilg H, Byrne CD, Targher G. Non-alcoholic fatty liver disease and risk of incident diabetes mellitus: an updated meta-analysis of 501 022 adult individuals. Gut. 2021;70:962–9.
6. Lim GEH, Tang A, Ng CH, Chin YH, Lim WH, Tan DJH, Yong JN, Xiao J, Lee CW-M, Chan M et al. An Observational Data Meta-Analysis on the differences in prevalence and risk factors between MAFLD vs NAFLD. Clin Gastroenterol Hepatology: Official Clin Pract J Am Gastroenterological Association. 2023;21.
7. Devarbhavi H, Asrani SK, Arab JP, Nartey YA, Pose E, Kamath PS. Global burden of liver disease: 2023 update. J Hepatol. 2023;79:516–37.
8. Buzzetti E, Pinzani M, Tsochatzis EA. The multiple-hit pathogenesis of non-alcoholic fatty liver disease (NAFLD). Metabolism. 2016;65:1038–48.
9. Friedman SL, Neuschwander-Tetri BA, Rinella M, Sanyal AJ. Mechanisms of NAFLD development and therapeutic strategies. Nat Med. 2018;24:908–22.
10. Takaki A, Kawai D, Yamamoto K. Multiple hits, including oxidative stress, as pathogenesis and treatment target in non-alcoholic steatohepatitis (NASH). Int J Mol Sci. 2013;14:20704–28.
11. Chen Z, Tian R, She Z, Cai J, Li H. Role of oxidative stress in the pathogenesis of nonalcoholic fatty liver disease. Free Radic Biol Med. 2020;152:116–41.
12. Sies H, Jones DP. Reactive oxygen species (ROS) as pleiotropic physiological signalling agents. Nat Rev Mol Cell Biol. 2020;21:363–83.
13. Zhang Q, Liu J, Duan H, Li R, Peng W, Wu C. Activation of Nrf2/HO-1 signaling: an important molecular mechanism of herbal medicine in the treatment of atherosclerosis via the protection of vascular endothelial cells from oxidative stress. J Adv Res. 2021;34:43–63.
14. Wang P, Zhang X, Zheng X, Gao J, Shang M, Xu J, Liang H. Folic acid protects against Hyperuricemia in C57BL/6J mice via ameliorating gut-kidney Axis Dysfunction. J Agric Food Chem. 2022;70:15787–803.
15. Meng M, Huo R, Wang Y, Ma N, Shi X, Shen X, Chang G. Lentinan inhibits oxidative stress and alleviates LPS-induced inflammation and apoptosis of BMECs by activating the Nrf2 signaling pathway. Int J Biol Macromol. 2022;222:2375–91.
16. Yao Y, Yim EKF. Fucoidan for cardiovascular application and the factors mediating its activities. Carbohydr Polym. 2021;270:118347.
17. Shiau J-P, Chuang Y-T, Cheng Y-B, Tang J-Y, Hou M-F, Yen C-Y, Chang H-W. Impacts of oxidative stress and PI3K/AKT/mTOR on metabolism and the future direction of investigating Fucoidan-modulated metabolism. Antioxid (Basel Switzerland). 2022;11.
18. Yin J, Wang J, Li F, Yang Z, Yang X, Sun W, Xia B, Li T, Song W, Guo S. The fucoidan from the brown seaweed Ascophyllum nodosum ameliorates atherosclerosis in apolipoprotein E-deficient mice. Food Funct. 2019;10:5124–39.
19. Xue M, Tian Y, Sui Y, Zhao H, Gao H, Liang H, Qiu X, Sun Z, Zhang Y, Qin Y. Protective effect of fucoidan against iron overload and ferroptosis-induced liver injury in rats exposed to alcohol. Biomed Pharmacotherapy = Biomedecine Pharmacotherapie. 2022;153:113402.
20. Shih P-H, Shiue S-J, Chen C-N, Cheng S-W, Lin H-Y, Wu L-W, Wu M-S. Fucoidan and Fucoxanthin Attenuate Hepatic Steatosis and inflammation of NAFLD through Modulation of Leptin/Adiponectin Axis. Mar Drugs. 2021;19.
21. Kim M-J, Jeon J, Lee J-S. Fucoidan prevents high-fat diet-induced obesity in animals by suppression of fat accumulation. Phytother Res. 2014;28:137–43.
22. Shen H, Cai S, Wu C, Yang W, Yu H, Liu L. Recent advances in three-Dimensional Multicellular Spheroid Culture and Future Development. Micromachines (Basel). 2021;12.
23. Xie R, Pal V, Yu Y, Lu X, Gao M, Liang S, Huang M, Peng W, Ozbolat IT. A comprehensive review on 3D tissue models: Biofabrication technologies and preclinical applications. Biomaterials. 2024;304:122408.
24. Wei F, Zhang X, Cui P, Gou X, Wang S. Cell-based 3D bionic screening by mimicking the drug-receptor interaction environment in vivo. J Mater Chem B. 2021;9:683–93.
25. Pingitore P, Sasidharan K, Ekstrand M, Prill S, Linden D, Romeo S. Human multilineage 3D spheroids as a model of liver steatosis and fibrosis. Int J Mol Sci. 2019;20.
26. Romualdo GR, Da Silva TC, de Albuquerque Landi MF, Morais JA, Barbisan LF, Vinken M, Oliveira CP, Cogliati B. Sorafenib reduces steatosis-induced fibrogenesis in a human 3D co-culture model of non-alcoholic fatty liver disease. Environ Toxicol. 2021;36:168–76.
27. Zhang J, Tan J, Wang M, Wang Y, Dong M, Ma X, Sun B, Liu S, Zhao Z, Chen L, et al. Lipid-induced DRAM recruits STOM to lysosomes and induces LMP to promote exosome release from hepatocytes in NAFLD. Sci Adv. 2021;7:eabh1541.
28. Zhang Q, Ma XF, Dong MZ, Tan J, Zhang J, Zhuang LK, Liu SS, Xin YN. MiR-30b-5p regulates the lipid metabolism by targeting PPARGC1A in Huh-7 cell line. Lipids Health Dis. 2020;19:76.
29. Li J, Wang T, Liu P, Yang F, Wang X, Zheng W, Sun W. Hesperetin ameliorates hepatic oxidative stress and inflammation via the PI3K/AKT-Nrf2-ARE pathway in oleic acid-induced HepG2 cells and a rat model of high-fat diet-induced NAFLD. Food Funct. 2021;12:3898–918.
30. Chu X, Zhou Y, Zhang S, Liu S, Li G, Xin Y. Chaetomorpha linum polysaccharides alleviate NAFLD in mice by enhancing the PPARalpha/CPT-1/MCAD signaling. Lipids Health Dis. 2022;21:140.
31. Fromenty B, Roden M. Mitochondrial alterations in fatty liver diseases. J Hepatol. 2023;78:415–29.
32. Abdelmalek MF. Nonalcoholic fatty liver disease: another leap forward. Nat Reviews Gastroenterol Hepatol. 2021;18:85–6.
33. Pirillo A, Casula M, Olmastroni E, Norata GD, Catapano AL. Global epidemiology of dyslipidaemias. Nat Reviews Cardiol. 2021;18:689–700.
34. Juan CA, de la Pérez JM, Plou FJ, Pérez-Lebeña E. The Chemistry of reactive oxygen species (ROS) revisited: outlining their role in Biological macromolecules (DNA, lipids and proteins) and Induced pathologies. Int J Mol Sci. 2021;22.
35. Kumar S, Duan Q, Wu R, Harris EN, Su Q. Pathophysiological communication between hepatocytes and non-parenchymal cells in liver injury from NAFLD to liver fibrosis. Adv Drug Deliv Rev. 2021;176:113869.
36. Lennicke C, Cochemé HM. Redox metabolism: ROS as specific molecular regulators of cell signaling and function. Mol Cell. 2021;81:3691–707.
37. Zheng H, Pei Y, Zhou C, Hong P, Qian Z-J. Amelioration of atherosclerosis in ox-LDL induced HUVEC by sulfated polysaccharides from Gelidium crinale with antihypertensive activity. Int J Biol Macromol. 2023;228:671–80.
38. Heeba GH, Morsy MA. Fucoidan ameliorates steatohepatitis and insulin resistance by suppressing oxidative stress and inflammatory cytokines in experimental non-alcoholic fatty liver disease. Environ Toxicol Pharmacol. 2015;40:907–14.
39. Sun Y, Xu M, Wang C, Guan S, Wang L, Cong B, Zhu W, Xu Y. Low-molecular-weight fucoidan bidirectionally regulates lipid uptake and cholesterol efflux through the p38 MAPK phosphorylation. Int J Biol Macromol. 2022;220:371–84.
40. Jin J-O, Yu Q. Fucoidan delays apoptosis and induces pro-inflammatory cytokine production in human neutrophils. Int J Biol Macromol. 2015;73:65–71.
41. Cheng Y, Gao Y, Li J, Rui T, Li Q, Chen H, Jia B, Song Y, Gu Z, Wang T, et al. TrkB agonist N-acetyl serotonin promotes functional recovery after traumatic brain injury by suppressing ferroptosis via the PI3K/Akt/Nrf2/Ferritin H pathway. Free Radic Biol Med. 2023;194:184–98.
42. Yamamoto M, Kensler TW, Motohashi H. The KEAP1-NRF2 system: a thiol-based sensor-effector Apparatus for maintaining Redox Homeostasis. Physiol Rev. 2018;98:1169–203.
43. Loboda A, Damulewicz M, Pyza E, Jozkowicz A, Dulak J. Role of Nrf2/HO-1 system in development, oxidative stress response and diseases: an evolutionarily conserved mechanism. Cell Mol Life Sci. 2016;73:3221–47.
44. Xiang Q, Zhao Y, Lin J, Jiang S, Li W. The Nrf2 antioxidant defense system in intervertebral disc degeneration: molecular insights. Exp Mol Med. 2022;54:1067–75.
45. Deng Z, Wu N, Suo Q, Wang J, Yue Y, Geng L, Zhang Q. Fucoidan, as an immunostimulator promotes M1 macrophage differentiation and enhances the chemotherapeutic sensitivity of capecitabine in colon cancer. Int J Biol Macromol. 2022;222:562–72.

46. Shiau JP, Chuang YT, Cheng YB, Tang JY, Hou MF, Yen CY, Chang HW. Impacts of oxidative stress and PI3K/AKT/mTOR on metabolism and the future direction of investigating Fucoidan-modulated metabolism. Antioxid (Basel). 2022;11.
47. Xue M, Ji X, Xue C, Liang H, Ge Y, He X, Zhang L, Bian K, Zhang L. Caspase-dependent and caspase-independent induction of apoptosis in breast cancer by fucoidan via the PI3K/AKT/GSK3beta pathway in vivo and in vitro. Biomed Pharmacother. 2017;94:898–908.
48. Liu Y, Xu Z, Huang H, Xue Y, Zhang D, Zhang Y, Li W, Li X. Fucoidan ameliorates glucose metabolism by the improvement of intestinal barrier and inflammatory damage in type 2 diabetic rats. Int J Biol Macromol. 2022;201:616–29.
49. Tacke F, Luedde T, Trautwein C. Inflammatory pathways in liver homeostasis and liver injury. Clin Rev Allergy Immunol. 2009;36.
50. Morgan MJ, Liu Z-g. Crosstalk of reactive oxygen species and NF-κB signaling. Cell Res. 2011;21:103–15.
51. Guo H, Guo H, Xie Y, Chen Y, Lu C, Yang Z, Zhu Y, Ouyang Y, Zhang Y, Wang X. Mo3Se4 nanoparticle with ROS scavenging and multi-enzyme activity for the treatment of DSS-induced colitis in mice. Redox Biol. 2022;56:102441.
52. Lee SM, Koh DH, Jun DW, Roh YJ, Kang HT, Oh JH, Kim HS. Auranofin attenuates hepatic steatosis and fibrosis in nonalcoholic fatty liver disease via NRF2 and NF- κB signaling pathways. Clin Mol Hepatol. 2022;28:827–40.
53. Wang X, Dong L, Dong Y, Bao Z, Lin S. Corn Silk flavonoids ameliorate hyperuricemia via PI3K/AKT/NF-κB pathway. J Agric Food Chem. 2023;71:9429–40.

Publisher's note